

## Synthesis and Characterization of $\text{La}_{0.8}\text{Sr}_{0.1}\text{Ag}_{0.1}\text{MnO}_3$ Nano Perovskite Compound

Abd El-Rahman T. AboZied<sup>1</sup>, Ahmed Abd El-Ghani<sup>2</sup>, Ahmed I. Ali<sup>3</sup>,  
TaHER Salah El-Din<sup>1,4</sup>

<sup>1</sup>Nanotechnology and Advanced Material Central Lab., ARC, Egypt.

<sup>2</sup>Physics Department, Ain Shams University, Egypt.

<sup>3</sup>Basic Science Department, Faculty of Industrial Education, Helwan University, Cairo, Egypt.

<sup>4</sup>British University in Egypt.

**Abstract:** Nano-crystalline perovskite of the general formula  $\text{La}_{0.8}\text{Sr}_{0.1}\text{Ag}_{0.1}\text{MnO}_3$  was synthesized using the Pechini sol-gel method. Variation of the gel pH was done during synthesis process to control the aggregation of particles and their crystal structural. The synthesized nanoparticles were characterized using X-ray analysis (XRD), High Resolution Transmission Electron Microscope (HR-TEM) and Thermal analyses (TGA/DTA). XRD confirms the formation of the pure phase perovskite in rhombohedral structure with R-3c space group and with crystallite size about 28 nm. The HR-TEM analysis further confirms the nanosize of the particles, which lie in the range of 35-40 nm. The magnetic hysteresis measurements were performed using a vibrating sample magnetometer (VSM). Magnetic parameters such as saturation magnetization, remanent magnetization, and coercivity were obtained. Based on the value of coercivity, this sample is good suited for data storage devices.

**Keywords:** Magnetic properties, Modern applications, Perovskite nanoparticles, Sol-gel process.

### I. Introduction

The hole-doped rare-earth perovskite manganites of general formula  $\text{RE}_{1-x}\text{A}_x\text{MnO}_3$  (RE = rare earth ion and A = divalent alkaline earth metal ion, Ca, Sr, Ba, Pb, etc. or monovalent alkaline metal ion, Na, Ag, K, ...), have spurred considerable scientific and technological interest in recent decades due to their remarkable magnetic, electric transport, catalytic and colossal magnetoresistance (CMR) properties, etc. [1-3].

Various wet-chemical methods have been developed to prepare high quality and homogenous products utilized in high technology applications. These methods are based on the principle that the reactants are mixed in the molecular level. Low calcination temperature is then needed to produce fine powders with higher surface area and high purity. In the present study, a Pechini-type polymerized complex route based on polyesterification between citric acid and ethylene glycol has been successfully used to synthesize perovskite nanometric sized powder. Ethylene glycol greatly inhibits metal ions segregation and achieves a homogeneous precursor in the polymerization of citric acid-metal complexes. [4, 5]. Some studies concerning the synthesis of other similar perovskite oxide materials by the mentioned methods have been reported, recently. [6, 7].

In this study, an effort has been made to synthesize the  $\text{La}_{0.8}\text{Sr}_{0.1}\text{Ag}_{0.1}\text{MnO}_3$  (LSAMO) in nano scale using mild sol-gel approach at a low temperature and further to investigate the influence of Sr and Ag (as a divalent – monovalent atoms substituted at A site respectively). The sol-gel is a preferable alternative method because it is very short reaction time, simple synthetic apparatus and simple operating procedure. This method also allows synthesis of LSAMO NPs in large scale up to several tenth grams. Thermogravimetric and Differential Thermal Analysis (TGA/DTA) has been investigated the sample to determine the sintering temperature. Moreover, XRD, TEM, and VSM were used for the characterization.

### II. Experimental

Powder sample with composition  $\text{La}_{0.8}\text{Sr}_{0.1}\text{Ag}_{0.1}\text{MnO}_3$  was prepared by sol-gel method. Analytical grade Lanthanum nitrate (III) Hexahydrate ( $\text{La}(\text{NO}_3)_3 \cdot 6\text{H}_2\text{O}$ ), Manganese nitrate Hexahydrate ( $\text{Mn}(\text{NO}_3)_2 \cdot 6\text{H}_2\text{O}$ ), Silver nitrate ( $\text{AgNO}_3$ ) and Strontium nitrate ( $\text{Sr}(\text{NO}_3)_2$ ) were taken in stoichiometric proportion and were dissolved in deionized water with subsequent addition of Citric acid and Ethylene Glycol. Afterwards, the monohydrate Citric acid and the Ethylene Glycol were added to ensure the homogeneity and the transparency of the solution. The ratio of Citric acid to total metal nitrates was 4:1. Ammonia was then added until the pH of the solution reached 6 and another mixture for pH equal 9. The mixture was then heated on a thermal plate under constant stirring at 120 °C to promote polymerization and to allow solvent removal. A viscous gel was thus obtained. After crushing, the sample was calcined at certain temperature determined from thermal analysis. With intermediate grinding, we obtained a fine nano-crystalline powder.

The phase purity, homogeneity and cell dimensions were determined by means of X-ray powder diffraction at room temperature with a diffractometer using  $\text{Cu K}\alpha$  radiation. The morphology and grain size distribution were studied by High Resolution Transmission Electron Microscope (HR-TEM, Tecnai G20, FEI, Netherland). The magnetic properties were investigated using a vibrating sample magnetometer (VSM) (Lake Shore model 7410) with field reach to 2T.

### III. Results and discussion

#### 3.1 Thermogravimetric and Differential Thermal Analysis (TGA/DTA)

In order to investigate the formation of the perovskite structure phase, thermal analyses are carried out in the temperature range 50 to 1000 °C using Thermogravimetric Analysis (TGA)/Differential Thermal Analysis (DTA).

**Fig.1** shows TGA and DTG for the  $\text{La}_{0.8}\text{Sr}_{0.1}\text{Ag}_{0.1}\text{MnO}_3$  sample. The DTG curve present an endothermic peak at the temperatures of 100 °C results from the loss of coordinated water. This process is accompanied by a sharp mass loss on the thermogravimetry (TG) curve. The exothermic one-step decomposition of the nitrate/citrate

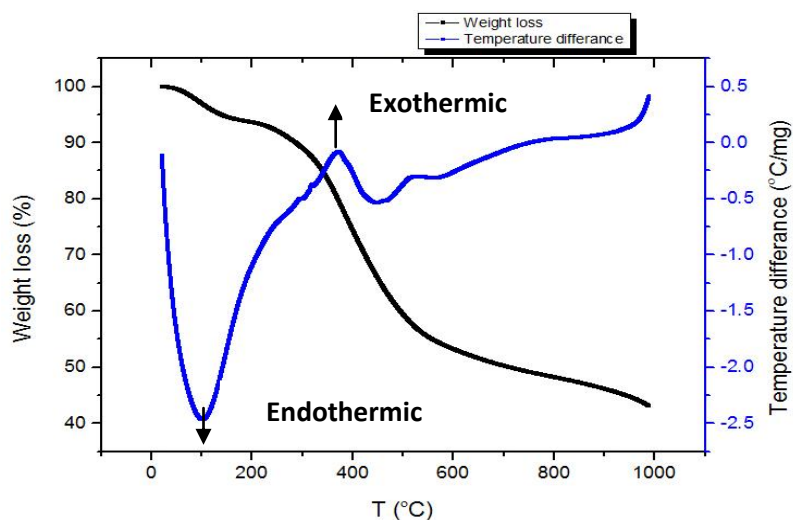


**Fig.1:** TGA/DTA for  $\text{La}_{0.8}\text{Sr}_{0.1}\text{Ag}_{0.1}\text{MnO}_3$  nanoparticles.

complexes takes place in the temperature range  $350\text{ °C} < T < 450\text{ °C}$ , which can be associated with the combustion reaction. Above 600 °C, there is no mass change in TGA curve suggesting the formation of perovskite phase which was also confirmed by XRD and HR-TEM. According to above data. We decided to sinter the sample at 800°C for more stability and crystallinity, according to the previous results.

#### 3.2 Structural properties

**Fig.2 (a-b)** presents the X-ray diffraction pattern of the  $\text{La}_{0.8}\text{Sr}_{0.1}\text{Ag}_{0.1}\text{MnO}_3$  sample prepared at different pH values (pH = 6 and 9). **Fig.2a** shows the XRD pattern of the sample prepared at controlled pH = 6. While **Fig.2b** shows the corresponding pattern at PH = 9. From both **Fig.2a** and **Fig.2b**, one can concluded that the crystallinity obtained at pH = 9 is much better than that obtained at pH = 6.

X-ray diffraction patterns (XRD) of **Fig.2b** shows the fundamentals peaks of the perovskite structure, which is appeared to be single-phase and crystallized in a rhombohedral perovskite structure with R3C space group. The lattice parameters are ( $a = 5.622\text{ Å}$ ) and ( $c = 13.904\text{ Å}$ ), which have been calculated using the relation [8]:

$$\frac{1}{d^2} = \frac{4}{3} \left( \frac{h^2 + hk + k^2}{a^2} \right) + \frac{l^2}{c^2}$$

where  $d_{hkl}$  is the inter-planer spacing (recorded automatically) and h, k and l are the Miller indices of each plane. The average crystallite size (D) of the  $\text{La}_{0.8}\text{Sr}_{0.1}\text{Ag}_{0.1}\text{MnO}_3$  sample lies in around 28 nm, which estimated from the XRD data using the Debye-Scherrer equation [9]:

$$D = \frac{K\lambda}{\beta \cos \theta}$$

where k is the crystallite factor (it was considered as 0.94),  $\lambda$  is the X-ray wavelength ( $\text{CuK}\alpha = 1.5406\text{ Å}$ ), and  $\beta$  is the peak full width at half maxima (in radians) at the observed peak angle  $\theta$ .

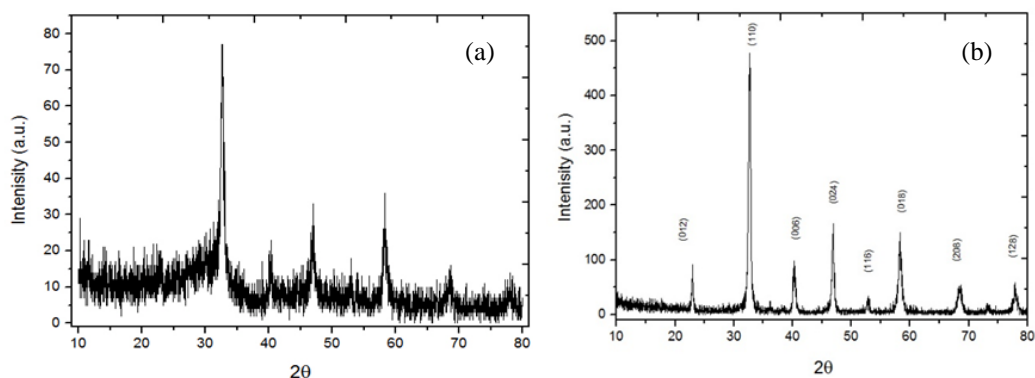


**Fig.2** a) XRD for  $\text{La}_{0.8}\text{Sr}_{0.1}\text{Ag}_{0.1}\text{MnO}_3$  nanoparticles at pH = 6, b) XRD for  $\text{La}_{0.8}\text{Sr}_{0.1}\text{Ag}_{0.1}\text{MnO}_3$  nanoparticles at pH = 9.

**Fig.3(a)** shows the HR-TEM photograph of the investigated sample at pH = 9. The photograph shows that the particles have nearly homogeneous distribution. The highly agglomerated state of the nanoparticles is due to their mutual magnetic interactions. It is evidenced by HR-TEM images that the aggregation of particles lies in nano metric region. The average particle sizes estimated from a large number of particles were found in the range of 39 nm, which differ a little bit from XRD results. This is because X-ray diffraction gives the data of crystalline region only and the contribution from the amorphous grain surface does not include. The particlesize distribution is given by the histograms shown in **Fig.3b**.

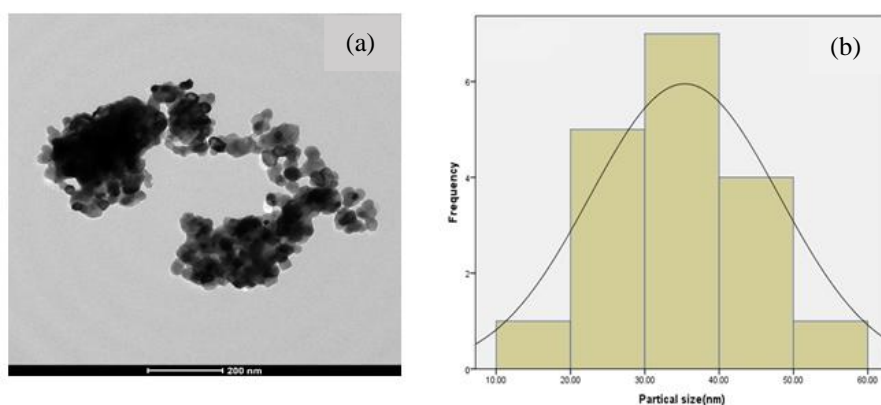


**Fig.3** a) HR-TEM for  $\text{La}_{0.8}\text{Sr}_{0.1}\text{Ag}_{0.1}\text{MnO}_3$  nanoparticles, b) Histogram for  $\text{La}_{0.8}\text{Sr}_{0.1}\text{Ag}_{0.1}\text{MnO}_3$  nanoparticles.

### 3.3 Magnetic properties

**Fig.4** displays the hysteresis loop of the investigated sample, which designates the soft nature of the sample. The sample exhibits very low coercivity values indicating that the sample belongs to the family of soft magnetic materials[10]. The values of the saturation magnetization ( $M_s$ ), coercivity ( $H_c$ ), retentivity ( $M_r$ ), energy loss and squareness ( $M_r/M_s$ ) are obtained and tabulated in **Table 1**. It is clear from the figure that the value of magnetization increases with increasing the applied field and gets saturated at a very low value of the applied field. The existence or absence of the different types of intergrain group exchanges is determined by the amount of  $M_r/M_s$  that varies from 0 to 1[11]. In our case the investigated sample have a magneto-static interaction. At the same time, the low value of the coercivity obtained qualifies the sample to be used in recording media to avoid the loss of the data bits[12].

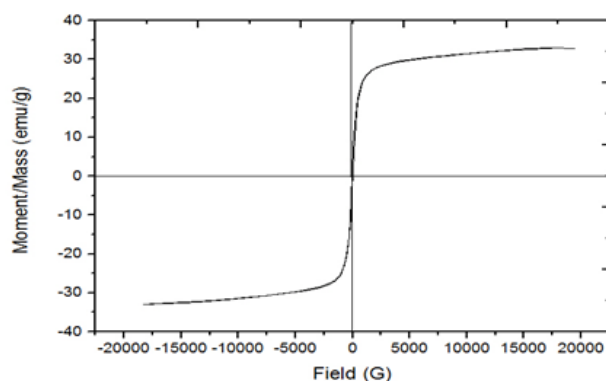


**Fig.4:** Hysteresis loop for  $\text{La}_{0.8}\text{Sr}_{0.1}\text{Ag}_{0.1}\text{MnO}_3$  nanoparticles.

**Table.1:** The values of the saturation magnetization ( $M_s$ ), retentivity ( $M_r$ ), coercivity ( $H_c$ ), energy loss and squareness ( $M_r/M_s$ ).

$\text{La}_{0.8}\text{Sr}_{0.1}\text{Ag}_{0.1}\text{MnO}_3$				
$M_s$ (emu/g)	$M_r$ (emu/g)	$H_c$ (Oe)	Energy loss (erg/g)	$M_r/M_s$
32.938	2.4725	37.283	7689.5	0.075

#### IV. Conclusion

In summary, we have fabricated  $\text{La}_{0.8}\text{Sr}_{0.1}\text{Ag}_{0.1}\text{MnO}_3$  nanoparticles by sol-gel method. The synthesized nanoparticles were characterized using XRD and HR-TEM. XRD confirms the formation of pure phase perovskite structure with rhombohedral symmetry in R-3C space group. By analyzing HR-TEM and XRD one can have nearly complete picture of the particle size, distribution of the particle size and the morphology. HR-TEM analysis supports the nanosized particles with grain size ranges from 35 to 40 nm. Based on the value of coercivity, this sample is good suited for data storage devices.

#### References

- [1]. Das, K., B. Satpati, and I. Das, *The effect of artificial grain boundaries on magneto-transport properties of charge ordered-ferromagnetic nanocomposites*. RSC Advances, 2015. **5**(35): p. 27338-27346.
- [2]. Sadhu, A. and S. Bhattacharyya, *Enhanced Low-Field Magnetoresistance in  $\text{La}_{0.71}\text{Sr}_{0.29}\text{MnO}_3$  Nanoparticles Synthesized by the Nonaqueous Sol-Gel Route*. Chemistry of Materials, 2014. **26**(4): p. 1702-1710.
- [3]. Venkataiah, G., et al., *Influence of Particle Size on Electrical Transport Properties of  $\text{La}_{0.67}\text{Sr}_{0.33}\text{MnO}_3$  Manganite System*. Journal of Nanoscience and Nanotechnology, 2007. **7**(6): p. 2000-2004.
- [4]. Liu, S., et al., *Synthesis of strontium cerates-based perovskite ceramics via water-soluble complex precursor routes*. Ceramics International, 2002. **28**(3): p. 327-335.
- [5]. Popa, M. and M. Kakhana, *Synthesis of lanthanum cobaltite ( $\text{LaCoO}_3$ ) by the polymerizable complex route*. Solid State Ionics, 2002. **151**(1-4): p. 251-257.
- [6]. Liu, S., K. Li, and R. Hughes, *Preparation of  $\text{SrCe}_{0.95}\text{Yb}_{0.05}\text{O}_{3-\alpha}$  perovskite for use as a membrane material in hollow fibre fabrication*. Materials Research Bulletin, 2004. **39**(1): p. 119-133.
- [7]. Popa, M., L.V. Hong, and M. Kakhana, *Nanopowders of  $\text{LaMeO}_3$  perovskites obtained by a solution-based ceramic processing technique*. Physica B: Condensed Matter, 2003. **327**(2-4): p. 233-236.
- [8]. Cullity, B.D. and S.R. Stock, *Elements of X-Ray Diffraction*. 3rd ed. 2014: Pearson Education Limited.
- [9]. Cullity, B.D., *Elements of X-ray Diffraction*. 2nd ed. 1978: Addison-Wesley Publishing Company Inc.
- [10]. Ateia, E.E. and A.T. Mohamed, *Nonstoichiometry and phase stability of Al and Cr substituted Mg ferrite nanoparticles synthesized by citrate method*. Journal of Magnetism and Magnetic Materials, 2017. **426**: p. 217-224.
- [11]. Kurtan, U., et al., *Temperature dependent magnetic properties of  $\text{CoFe}_2\text{O}_4/\text{CTAB}$  nanocomposite synthesized by sol-gel auto-combustion technique*. Ceramics International, 2013. **39**(6): p. 6551-6558.
- [12]. Saranu, S., et al., *Effect of large mechanical stress on the magnetic properties of embedded Fe nanoparticles*. Beilstein Journal of Nanotechnology, 2011. **2**: p. 268-275.